Materials Science for Energy Technologies 2 (2019) 385–388

Contents lists available at ScienceDirect

Materials Science for Energy Technologies

journal homepage: www.keaipublishing.com/en/journals/materials-science-for-energy-technologies

Effect of doped TiO_2 film as electron transport layer for inverted organic solar cell

A. Ranjitha [a,*], M. Thambidurai [b], Foo Shini [c], N. Muthukumarasamy [d], Dhayalan Velauthapillai [e]

[a] Department of Physics, Kongunadu Arts and Science College, India
[b] LUMINOUS! Centre of Excellence for Semiconductor Lighting and Displays, School of Electrical & Electronic Engineering, Nanyang Technological University, 50 Nanyang Avenue, 639798, Singapore
[c] School of Materials Science and Engineering, Nanyang Technological University, 50 Nanyang Avenue, 639798, Singapore
[d] Department of Physics, Coimbatore Institute of Technology, India
[e] Western Norway University of Applied Sciences, Department of Computing, Mathematics and Physics, Bergen, Norway

ARTICLE INFO

Article history:
Received 22 January 2019
Revised 21 February 2019
Accepted 26 February 2019
Available online 16 March 2019

Keywords:
Doped TiO_2
Polymer solar cells
Sol–gel method
XRD

ABSTRACT

Nanocrystalline TiO_2 and Sn-doped TiO_2 thin films were prepared by sol–gel spin coating method. The crystallinity and anatase phase of TiO_2 and Sn-doped TiO_2 were confirmed from X-ray diffraction analysis. The EDAX analysis also confirmed the presence of tin, oxygen and titania elements. By fabricating an inverted organic solar cell with device configuration of ITO/Sn-doped TiO_2/active layer/MoO_3/Al, power conversion efficiency (PCE) of the Sn-doped TiO_2 was observed to be 3.08% compared to the TiO_2 based solar cell of 2.64%.

1. Introduction

Titanium dioxide has been commonly employed as a suitable buffer layer due to its chemical stability and non-toxicity. As such, n-type metal oxides such as TiO_x are often utilized as a stable n-type buffer layer in applications such as organic photovoltaics [1–5], photocatalysis, electrocatalytic [6], dye sensitized solar cells [7], lithium ion batteries [8], and polymer solar cells [9–13]. Recently, several reports have shown the applicability of solution based ZnO [14,15,16] and TiO_x [17,18] layers as efficient electron transport layers in organic solar cells, achieving high power conversion efficiencies (PCEs). Meanwhile, Zimmermann et al. [19] and Hsieh et al. [20] have reported the stability of active layer P3HT:PCBM. The electrical and optical properties of TiO_2 are commonly attributed to the presence of impurities and oxygen vacancies. Thus, incorporation of impurity atoms into the TiO_2 lattice without changing the crystallographic structure is often viewed as a simple yet effective approach to improve the properties of TiO_2.

Considerable interest has been focused on metal doping and is found as an effective procedure to modify the conductivity, electrical and optical properties of n-type buffer layer [21]. Zuhal et al. [22] doped Mn^{2+}into the TiO_2 lattice for organic hybrid solar cell applications. Doping Sn into TiO_2 is an attractive method to ensure good stability and structural compatibility due to the small mismatch of band gap between SnO_2 and TiO_2 [23]. Since SnO_2 and TiO_2 are both wide band gap semiconductors with the former having a larger band gap of 3.8 eV than the latter of 3.2 eV. Also, SnO_2 has a lower fermi level than TiO_2 [24]. Furthermore, the addition of Sn or SnO_2 into the TiO_2 lattice is reported to facilitate shifting in the band edge of TiO_2 [25,26]. On the other hand, the formation of SnO_2/TiO_2 core-shell nanoparticles [27] is reported to greatly reduce the exciton recombination. In this study, simple sol–gel approach is utilized to synthesize nanocrystalline Sn-doped TiO_2 electron selective thin film. The inverted polymer solar cells with device configurations of ITO/TiO_2/P3HT:$PC_{71}BM$/MoO_3/Al and ITO/Sn-doped TiO_2/P3HT:$PC_{71}BM$/MoO_3/Al were fabricated. Device characteristics and performances were then compared and studied.

* Corresponding author.
E-mail address: ranjichitra@gmail.com (A. Ranjitha).

Peer review under responsibility of KeAi Communications Co., Ltd.

Production and hosting by Elsevier

https://doi.org/10.1016/j.mset.2019.02.006
2589-2991/

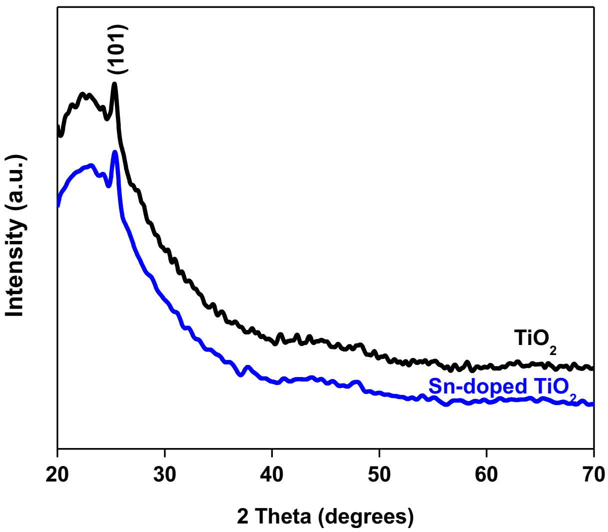

Fig. 1. X-ray diffraction pattern of TiO_2 and Sn-doped TiO_2 thin films.

2. Experimental procedure

Sn-doped TiO_2 films was fabricated by mixing titanium (IV) butoxide, tin (II) chloride ($SnCl_2{\cdot}2H_2O$), and acetyl acetone in 2-Methoxyethanol without heating. The well-mixed and transparent solution was then spun on the ITO substrate to form the respective un-doped and Sn-doped TiO_2 ETLs before annealing at 500 °C for an hour to remove organic residues as well as allow film densification. The coated substrates were then transferred into a nitrogen-filled glove box for further spin coating of the organic active layer made from the P3HT and $PC_{71}BM$ blend at a ratio of 1:0.8 in chlorobenzene. After which, a thin layer of 10 nm and 100 nm of MoO_3 and Al were thermally evaporated using a shadow mask under pressure of 10^{-6} torr, respectively.

Structural properties of prepared samples were identified by X-Ray Diffraction (XRD) technique using XPERT-PRO X-Ray Diffractometer system. On other hand, morphology analysis and compositional analysis were carried out using Zeiss supra 55VP FESEM and Energy Dispersive Analysis X-Ray. JASCO V570 spectrophotometer was utilized to understand the optical properties of the films. Current density-voltage (J-V) characteristics was measured using the Keithley 237 m coupled with a 1.5G solar simulator (Newport, 91160A) and a xenon lamp source irritated at 100 mW/cm^2 Am.

3. Results and discussion

Fig. 1 shows XRD patterns of TiO_2 and Sn-doped TiO_2 thin films. Both patterns depict the fabrication of the TiO_2 anatase phase. Also, the XRD results showed negligible effect of Sn doping on the TiO_2 crystal structure. In addition, since the thickness of TiO_2 (30 nm) is low, only the dominant (1 0 1) peak was observed in the XRD pattern. Signals for the other peaks are too low and cannot be detected using XRD as seen in other references too [28,29]. Scherrer's equation was used to calculate the grain size of the prepared films.,

$$D = \frac{K\lambda}{\beta \mathrm{Cos}\theta},$$

where D is the grain size, while K takes a value of 0.94, λ corresponds to wavelength of X-ray radiation, β represents the full width at half maximum (FWHM), and θ is the angle of diffraction. According to the FWHM of the (1 0 1) diffraction peak, the grain size was calculated to be 37 nm and 32 nm for TiO_2 and 2% Sn-doped TiO_2 samples, respectively. The decrease in grain size could be explained by the absorption of Sn^{4+} into the TiO_2 nucleus since SnO_2 and TiO_2

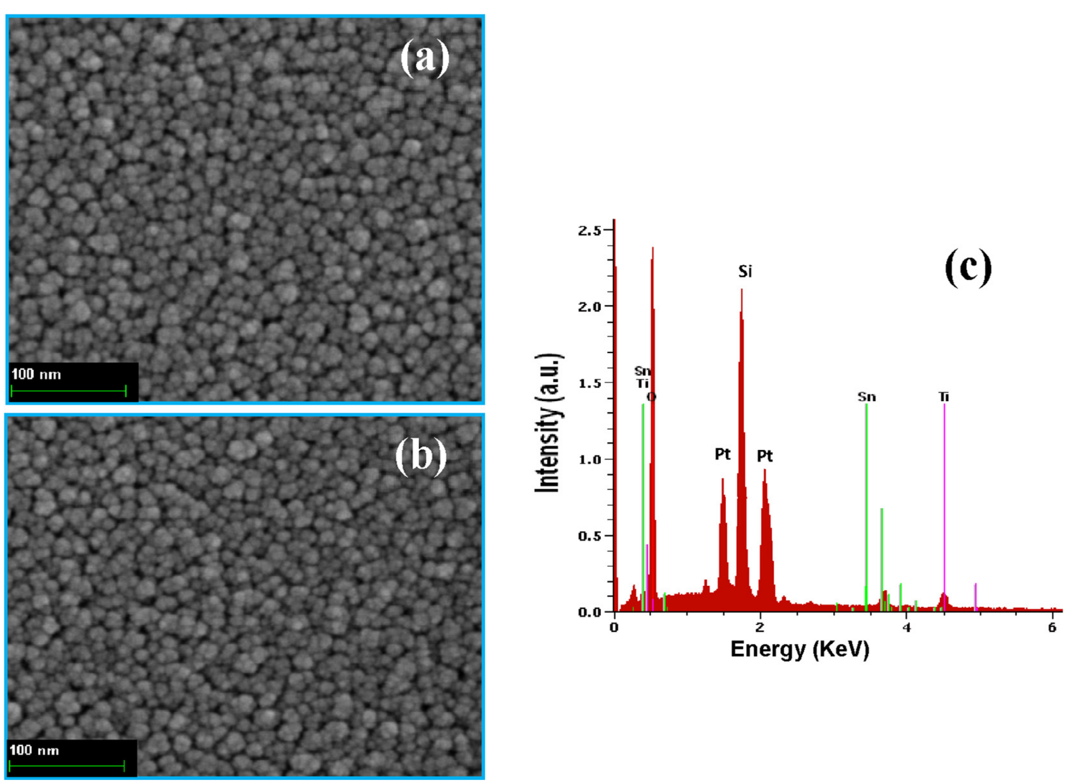

Fig. 2. FESEM images of (a) TiO_2 and (b) Sn-doped TiO_2 thin films. (c) EDAX spectra of Sn-doped TiO_2 thin film.

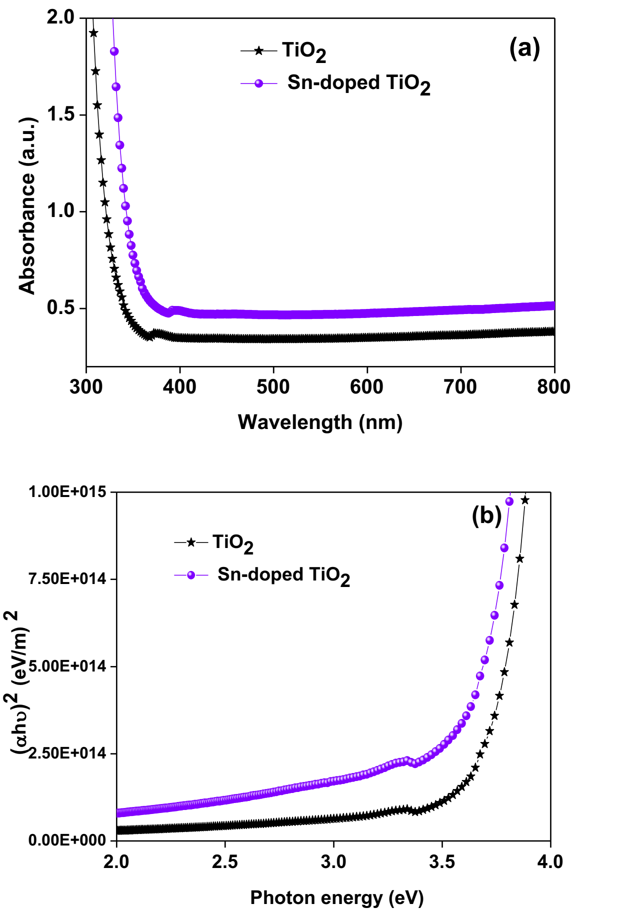

Fig. 3. (a) Optical absorption spectra and (b) plot of $(\alpha h\upsilon)^2$ versus $h\upsilon$ of TiO_2 and 2% Sn-doped TiO_2 films.

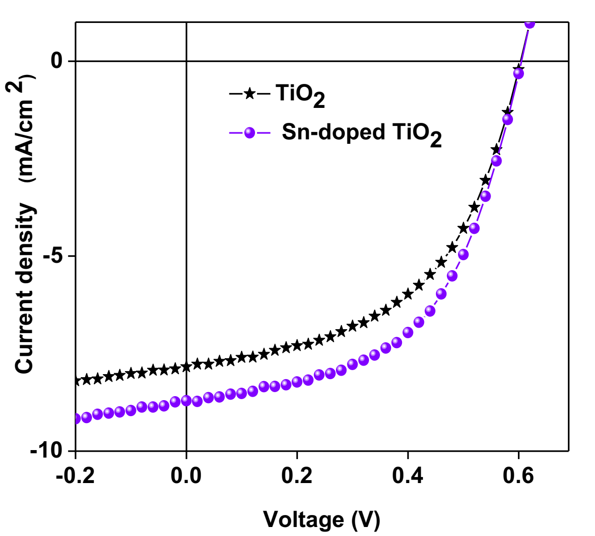

Fig. 4. J–V characteristics of TiO_2 and 2% Sn-doped TiO_2 based polymer solar cells.

have the same crystal structure hence retarding growth of TiO_2 particles, resulting in the decrease in grain size.

Fig. 2(a,b) shows the surface morphology of TiO_2 and 2% Sn-doped TiO_2 thin films whereby both films display smooth morphologies with uniformly distributed. With a smoother surface, better interfacial contact arises between active layer and electron transport layer, which could benefit efficient of electron collection.

Fig. 2c shows the EDAX spectrum of 2% Sn-doped TiO_2 thin film in which Ti, O, and Sn were identified. The presence of Sn shows direct evidence that TiO_2 thin film has been doped with Sn.

The absorption spectra of TiO_2 and 2% Sn-doped TiO_2 films are shown in Fig. 3a. According to Fig. 3a, the addition of Sn results in slight shifting of absorption edge towards shorter wavelength compared to undoped film. Also, the conduction band bottom and top of the valence band is relatively higher in the TiO_2 film compared to SnO_2. Hence, photo-generated holes move to the surface of TiO_2. The presence of effective charge separation decreases the rate of recombination while induces effective charge separation since there are a large amount of contact sites as seen from SEM analysis. The relationship between absorption co-efficient (α) and incident photon energy ($h\nu$) is given as,

$$(\alpha h\upsilon) = A(h\upsilon - E_g)^n,$$

where A is a constant and h represents the Planck's constant. Also, E_g, ν and exponent n corresponds to band gap, frequency of incident radiation, and 0.5 for direct allowed transitions, respectively [30]. Fig. 3b shows plot of $(\alpha h\nu)^2$ verses $h\nu$. The optical band gap of TiO_2 and 2% Sn-doped TiO_2 films were determined via the above relation. By extrapolating the linear portion of the plot to energy axis, the band gap energy was found to be 3.4 eV and 3.5 eV for TiO_2 and 2% Sn-doped TiO_2 films, respectively. This shows that higher energy band gap induces lower rate of recombination.

Current density-voltage characteristics of the as-fabricated inverted organic solar cells are shown in Fig. 4. The TiO_2 based ETL device exhibited short circuit current density (J_{sc}) of 7.91 mA cm^{-2}, open circuit voltage (V_{oc}) of 0.64 V, fill factor (FF) of 0.51, and efficiency (η) of 2.64%. On the other hand, 2% Sn-doped TiO_2 exhibited 8.84 mA cm^{-2}, 0.64 V, 0.54 of J_{sc}, V_{oc}, FF and η of 3.08%. The device incorporated with the Sn-doped TiO_2 electron transport layer (ETL) showed enhancement in device performance in which the doped ETL showed higher Jsc. Also, effective charge separation was observed since the TiO_2 and Sn particles were well mixed and provided a lot of contact sites. Furthermore, the improved electrical properties could be attributed to the replacement of Ti^{4+} with Sn^{4+}. This could be explained by the smaller radius of Sn^{4+} is larger than that of Ti^{4+} cation, resulting in the decrease in particle size and increase in band gap.

4. Conclusion

Nanocrystalline TiO_2 and 2% Sn-doped TiO_2 thin films were prepared by simple sol–gel method. The prepared films were characterized by XRD, FESEM, EDAX, and J-V characterization. The nature of doping in small amount enabled retainment of crystal structure. Unlike the undoped TiO_2 thin film, the inverted organic solar device containing 2% Sn-doped TiO_2 ETL showed significant improvement in PCE of 3.08% compared to the undoped device of 2.64%.

Conflict of interest

The authors declare that there is no conflict of interest.

References

[1] R. Steim, R. Kogler, C.J. Brabec, Interface materials for organic solar cells, J. Mater. Chem. 20 (2010) 2499–2512.

[2] H. Oh, J. Krantz, I. Litzov, T. Stubhan, L. Pinna, C.J. Brabec, Comparison of various sol-gel derived metal oxide layers for inverted organic solar cells, Sol. Energy Mater. Sol. Cells 95 (2011) 2194–2199.

[3] Johannes Lockinger, Shiro Nishiwaki, Thomas P. Weiss, Benjamin Bissig, Yaroslav E. Romanyuk, Stephan Buecheler, Ayodhya N. Tiwari, TiO_2 as intermediate buffer layer in Cu(In, Ga)S_e2 solar cells, Sol. Energy Mater. Sol. Cells 174 (2018) 397–404.

[4] Teddy Salim, Zongyou Yin, Shuangyong Sun, Xiao Huang, Hua Zhang, Yeng Ming Lam, Solution-processed Nanocrystalline TiO_2 Buffer layer used for improving the performance of organic photovoltaics, ACS Appl. Mater. Interfaces 3 (2011) 1063–1067.
[5] Kai Wang, Chang Liu, Tianyu Meng, Inverted organic photovoltaic cells, Chem. Soc. Rev. 45 (2016) 2937–2975.
[6] Akshatha R. Shetty, Ampar Chitharanjan Hegde, Effect of TiO_2 on electrocatalytic behaviour of Ni-Mo alloy coating for hydrogen energy, Mater. Sci. Energy Technol. 1 (2018) 97–105.
[7] T. Solaiyammal, P. Murugakoothan, Green synthesis of Au and the impact of Au on the efficiency of TiO_2 based dye sensitized solar cell, Mater. Sci. Energy Technol. (2019), https://doi.org/10.1016/j.mset.2019.01.001.
[8] Amit Mishra, Akansha Mehta, Soumen Basu, Shweta J. Malode, Nagaraj P. Shetti, Shyam S. Shukla, Mallikarjuna N. Nadagouda, Tejraj M. Aminabhavi, Electrode materials for lithium-ion batteries, Materials Science for, Energy Technol. 1 (2018) 182–187.
[9] M.R. Hoffmann, S.T. Martin, W. Choi, D.W. Bahnemann, Environmental applications of semiconductor photocatalysis, Chem. Rev. 95 (1995) 69–96.
[10] D.L. Liao, B.Q. Liao, Shape, size and photocatalytic activity control of TiO_2 nanoparticles with surfactants, J. Photochem. Photobiol. A: Chem. 187 (2007) 363–369.
[11] K. Shankar, J. Bandara, M. Paulose, H. Wietasch, O.K. Varghese, G.K. Mor, T.J. LaTempa, M. Thelakkat, C.A. Grimes, Highly efficient solar cells using TiO_2 nanotube arrays sensitized witha donor-antenna dye, Nano Lett. 8 (2008) 1654–1659.
[12] D. Kuang, J. Brillet, P. Chen, M. Takata, S. Uchida, H. Miura, K. Sumioka, S.M. Zakeeruddin, M. Gratzel, Application of highly ordered TiO_2 nanotube arrays in flexible dye-sensitized solar cells, ACS Nano 2 (2008) 1113–1116.
[13] S.W. Kim, T.H. Han, J. Kim, H. Gwon, H.S. Moon, S.W. Kang, S.O. Kim, K. Kang, Fabrication and electrochemical characterisation of TiO_2 three-dimensional nanonetwork based on pepetide assembly, ACS Nano 3 (2009) 1085–1090.
[14] Bobak Gholamkhass, Nima Mohseni Kiasari, Peyman Servati, An efficient inverted organic solar cell with improved ZnO gold contact layers, Org. Electron. 13 (6) (2012) 945–953.
[15] M. Thambidurai, Jun Young Kim, Jiyun Song, Youngjun Ko, N. Muthukumarasamy, Dhayalan Velauthapillai, Changhee Lee, Nanocrystalline Ga-doped ZnO thin films for inverted polymer solar cells, Solar Energy 106 (2014) 95–101.
[16] M. Thambidurai, Jun Young Kim, Chan-mo Kang, N. Muthukumarasamy, Hyung-Jun Song, Jiyun Song, Youngjun Ko, Dhayalan Velauthapillai, Changhee Lee, Enhanced photovoltaic performance of inverted organic solar cells with In-doped ZnO as an electron extraction layer, Renewable Energy 66 (2014) 433–442.
[17] A.L. Hashimi, K. Mohammed, K. Kadem, Y. Burak, Hassan K. Aseel, Rutile TiO_2 films as electron transport layer in inverted organic solar cell, J. Mater.Sc.: Mater. Electron. 29 (2018) 7152–7160.
[18] A. Ranjitha, N. Muthukumarasamy, M. Thambidurai, Dhayalan Velauthapillai, A. Madhan Kumar, Zuhair M. Gasem, Inverted organic solar cells based on Cd-doped TiO_2 as an electron extraction layer, Superlattices Microstruct. 74 (2014) 114–122.
[19] B. Zimmermann, U. Würfel, M. Niggemann, Longterm stability of efficient inverted P3HT:PCBM solar cells, Solar Energy Mater. Solar Cells 93 (2009) 491–496.
[20] C.H. Hsieh, Y.J. Cheng, P.J. Li, C.H. Chen, M. Dubosc, R.M. Liang, C.S. Hsu, Highly efficient and stable inverted polymer solar cells integrated with a cross-linked fullerene material as an interlayer, J. Am. Chem. Soc. 132 (2010) 48874893.
[21] Mi-Hyae Park, Juo-Hao Li, Ankit Kumar, Gang Li, Yang Yang, Doping of the metal oxide nanostructure and its influence in organic electronics, Adv. Funct. Mater. 19 (2009) 1241–1246.
[22] Zuhal Alparslan, Arif Kosemen, Osman Ornek, Yusuf Yerli, S. Eren, TiO_2-Based organic hybrid solar cells with Mn^{+2} doping, Int. J. Photoenergy (2011), https://doi.org/10.1155/2011/734618.
[23] Y.C. Ling, G.M. Wang, D.A. Wheeler, J.Z. Zhang, Y. Li, Sn-doped hematite nanostructures for photoelectrochemical water splitting, Nano Lett. 11 (2011) 2119–2125.
[24] B.F. Xin, D.D. Ding, Y.N. Gao, X.G. Jin, H. Fu, P. Wang, Preparation of nanocrystalline Sn-TiO_2-X via a rapid and simple stannous chemical reducing route, App. Surf. Sci. 255 (2009) 5896–5901.
[25] F. Sayılkan, M. Asilturk, P. Tatar, N. Kiraz, S. Sener, E. Arpac, H. Sayılkan, Photocatalytic performance of Sn-doped TiO_2 nanostructured thin films for photocatalytic degradation of malachite green dye under UV and VIS-lights, Mater. Res. Bull. 43 (2008) 127–134.
[26] K. Vinodgopal, I. Bedja, P.V. Kamat, Nanostructured semiconductor films for photocatalysis. Photoelectrochemical behaviour of SnO_2/TiO_2 composite systems and its role in photocatalytic degradation of a textile azo dye, Chem. Mater. 8 (1996) 2180–2187.
[27] J. Pan, S.M. Huhne, H. Shen, L.S. Xiao, P. Born, W. Mader, S. Mathur, SnO_2-TiO_2 core-shell nanowire structures: investigations on solid state reactivity and photocatalytic behaviour, J. Phy. Chem. C 115 (2011) 17265–17269.
[28] G. Govindasamy, P. Murugasen, S. Sagadevan, Investigations on the synthesis, optical and electrical properties of TiO_2 thin films by chemical bath deposition (CBD) method, Mater. Res. 19 (2) (2016) 413–419.
[29] A.K. Singh, S.B. Patil, U.T. Nakate, K.V. Gurav, Effect of Pd and Au sensitization of bath deposited flowerlike TiO_2 thin films on CO sensing and photocatalytic properties, J. Chem. 2013 (2013) 1–8.
[30] M. Thambidurai, N. Muthukumarasamy, Dhayalan Velauthapillai, S. Agilan, R. Balasundaraprabhu, Structural, optical, and electrical properties of cobalt-doped CdS quantum dots, J. Electron. Mater. 41 (2012) 665–672.